New Materials, Compounds and Applications
Vol.1, No.1, 2017, pp.65-93

FORMATION OF THE HYDROPHOBIC SURFACE OF THE BALL-SHAPED TITANIUM HEAD OF THE HUMAN HIP JOINT ENDOPROSTHESIS BY DIRECT LASER IRRADIATION

Sharif E. Guseynov[1,2,3*], Jekaterina V. Aleksejeva[1], Anita Jansone[1,2], Dace Kuma[2]

[1]Institute of Fundamental Science and Innovative Technologies, Liepaja, Latvia
[2]Faculty of Science and Engineering, Liepaja University, Liepaja, Latvia
[3]"Entelgine" Research & Advisory Co., Ltd., Riga, Latvia

Abstract. One of the most promising ways of periodic and/or nonperiodic nanostructure formation on implants' material surface, particularly on titanium surface, providing the implants with the desired adhesive and wettability properties is direct laser nanostructuring which uses only a laser beam with no atomic-force microscope's ancillary needle or masks in order to form surface nanorelief. In the present paper, the model of nanostructure formation on solid surface by microsecond laser pulses melting the material is described. It is shown that typical size of surface nanostructure formed depends on laser wavelength, pulse energy, pulse repetition rate, and pulse duration. Within the present work a series of 12 experiments devoted to direct laser nanostructuring of titanium and copper surfaces is carried out. Besides, the effects of nanoroughness on the contact and sliding angles on hydrophobic and hydrophilic surfaces were studied theoretically and experimentally.

Keywords: *nanostructured hydrophobic surface, hysteresis of contact angle, wetting properties, surface energy, laser irradiation.*

Corresponding Authors: *Dr.Sc.Math., Professor Sharif E. Guseynov, Liepaja University, Faculty of Science and Engineering, Institute of Fundamental Science and Innovative Technologies, 4 Kr.Valdemar Street, Liepaja LV-3401, Latvia, Tel.: (+371)22341717, e-mail: sh.e.guseinov@inbox.lv*

Manuscript received: *22 October 2017*

1. Introduction. Artificial materials to replace damaged tissues, bones and organs

At the present time nanostructures are paid additional attention for being an extremely promising object regarding its application in different fields of science, technology and medicine. Surface nanostructuring leads to improvement of nanotribological (Eletskii et al., 2012), thermalphysic and thermodynamic (Cao, 2004), electron-emission (Bhushan, 1994) properties of materials, promotes rise of implants' biocompatibility (Hao & Lawrence, 2005; Oshida, 2013; Remeeva et al., 2003) as well as leads to desired alteration of adhesive properties (Israelachvili, 1992; Khomich & Shmakov, 2012; Majumder et al., (2007) and wettability (Ferrara et al., 2010; Rios et al., 2006). One of the most promising ways of nanostructure formation on implants' material surface, particularly on titanium surface, providing the implants with the desired adhesive and wettability properties, is direct laser nanostructuring (see Khomich et al., 2013; Kendall, 1994) and respective references given in these) which uses only a laser beam with no atomic-force microscope's ancillary needle or masks in order to form surface nanorelief. The advantage of this method consists in its simplicity and flexibility:

- use of a single laser beam of a small size allows to achieve a high locality of exposure corresponding to the size (100x100 micrometer) of a separate laser spot;
- use of software-programmable laser beam scanning on the implants' material surface with a high irradiation pulse repetition frequency allows to nanostructure sufficiently large surface areas within almost arbitrary boundaries with high spatial resolution.

This work, which in some sense is a continuation of the work (Zaimis & Guseynov, 2017), is devoted to formation of hydrophobic nanostructure on the surface of a ball-shaped titanium head of the human hip joint endoprosthesis using direct laser nanostructuring. In this work, following the work (Adamson & Gast, 1997), we will consider that a partially hydrophilic or hydrophobic surface with respect to any fluid is such a solid surface that for it the fluid gives a finite contact angle:

- if the contact angle θ between a drop of the liquid and the solid surface varies in the interval $\left(0, \frac{\pi}{2}\right)$, then this surface is called hydrophilic;
- if $\theta \in \left(\frac{\pi}{2}, \frac{5 \cdot \pi}{6}\right]$, then the surface is called hydrophobic;
- if $\theta \in \left(\frac{5 \cdot \pi}{6}, \pi\right]$, then the surface is classified as ultra-hydrophobic, and such type surface combines natural hydrophobicity with roughness, which leads to practically complete non-wetting;
- if $\theta = 0$ or $\theta = \pi$ we have complete wettability or complete nonwettability of the surface, respectively.

Hydrophobic and ultra-hydrophobic materials have unique functional properties: for example, water resistance, corrosion resistance, resistance to biofouling, resistance to inorganic and organic contamination, etc. Near the hydrophobic surface of such materials, the slippage of fluid flow is heightened (including blood, body fluids and serum, etc.). Generally speaking, it can be said that hydrophobia is a property that is largely determined not by the physical characteristics of the material itself as a whole, but by the properties and structure of the near-surface layer in thickness of several nanometers. Consequently, for the production of hydrophobic and ultra-hydrophobic materials it is necessary to carry out a deep analysis of the processes that occur in nano-sized systems. One of such important processes is the hydrodynamics of liquids in thin channels in the diameter of the micron scale: the laws of the flow of liquids in microscale channels are very different from the classical laws of hydrodynamics, and the superficial effects play a huge role in the behavior of the liquid (see Ajdari, 1995; Vinogradova & Yakubov, 2006) and corresponding references given there).According to the theory, it is precisely the flow of fluid in the channels along the gas phase, which achieves the maximal fluid velocity at the wall. Therefore, the problem of the stability of such a state is one of the most important in manufacturing of ultra-hydrophobic surfaces. For ultra hydrophobic surfaces, there are two main thermodynamic states: the state of Wenzel (Wenzel, 1936), in which the cavity (i.e. thin channels) of the surface layer is filled with liquid; the state of Cassie (see Baxter & Cassie, 1945; Cassie & Baxter, 1945 as well as Gong, 2013), in which the cavities are filled with gas and, consequently, the contact of the liquid with the wall is a heterogeneous interfacial

liquid-solid state gas. It should be noted here that the study of the stability of the Cassie state is a key problem not only in microscale hydrodynamics, but also in many other applications. In principle, by arranging the texture (i.e. relief, topology) of the ultra-hydrophobic surface, it is quite possible to control the process of stabilizing the gas bubbles inside the cavities. However, in spite of the large number of theoretical and experimental studies (for instance, see Barrat & Bocquet, 1999; Belyaev & Vinogradova, 2010; Choi et al., 2003; Cottin-Bizonne et al., 2004; Lauga & Stone, 2003; Oner, 2001; Oner & McCarthy, 2000; Ou & Rothstein, 2005; Steinberger et al., 2007; Vinogradova & Yakubov, 2006; Ybert et al., 2007) and corresponding references given there), by now, the question of choosing such a topology of a surface at which slipping of the liquid on the surface will be maximal, has not been studied to fully and remains an open question.

Modern medicine widely uses artificial materials to replace damaged tissues, bones and organs. Depending on their purpose, the implants involved into the body should be gradually replaced with a living tissue and / or to function for a long time period. The tissue composition of the human bone has a complex structure. The mechanical strength of bone tissue is based on spatial arrangement of the structural components of bones – bone plates. The composition of the bone includes an organic component – collagen (≈25%), inorganic component – calcium phosphates (≈65%), water (≈10%) (see Puz, 2014). Artificial materials claiming the role of implants must meet the requirements dictated by the composition and properties of human bone tissue. The main requirements for artificial materials for implantation are resistance to corrosive media and biomechanical compatibility. In addition, the implant material must also posse some mechanical properties, of which the most prestigious are hardness, tensile strength and modulus of elasticity. Since the response of any material to repeated cyclic loads depends on the fatigue strength of the material, it is the property, that determines the continues usage time of the implant (see Hench, 1998). Because of the fact that the human body is an aggressive environment for implants, especially those made of metals, when developing new implants, it is necessary to take into account not only their functional characteristics, but also their interaction with the biological environment in where they will be used in. Low wear resistance and low corrosion resistance of metal implants in the corrosive liquid medium of the human body promote the release of metal ions into the body. It has been found (see Cardaioli et al., 2007) that Ni^{2+}, Co^{3+}, Al^{3+}, Cr^{3+} ions cause allergic and toxic reactions in the body, and therefore materials used as implants should not have toxicity or should have reliable protective coatings on surfaces that prevent Release of metal ions in the tissues of the human body. For small-size implants, pitting corrosion also poses a risk: for example, the functional integrity of the vascular walls can be destroyed by the presence of only one minor deepen.

On the surface and boundaries of the implant and soft tissues of the body undergo chemical and biological processes, carried out, in particular, on the cell-matrix and nanoscale level. The search for new biocompatible materials with nanostructured characteristics has been implementing according to the biomimetic approach, according to which artificial nanomaterials mimic the properties of biomaterials from living nature. Qualitative progress in this area is possible only based on interdisciplinary research in medicine, chemistry, biology, materials science, physics and mathematics. Since the 60s of the XX century, specialists in the areas listed above work closely together to understand the complex processes of interaction of body cells with the

foreign surface of the implanted material. Biologically active properties of the interface between the tissues of the body and the implanted material reviewed in correlation with its specific properties. The chemical composition of the surface, its physical and chemical characteristics, roughness and morphology, the determination of the activity of various cellular structures acting separately and synergistically are studied. The relationship between the physical and chemical properties of the surface and the cellular response is far from to be clear (for instance, see Cardaioli et al., 2007; Gintsburg et al., 2011; Hench, 1998; Puz, 2014; Rozenberg et al., 2006; Takemoto et al., 2004; Turmanidze et al., 2015) and respective references given in these). A firm understanding of the mechanism of this connection will lead to the creation of a new generation of materials that can be more effectively and successfully involvedinto the human body for therapeutic purposes. The classical concept of bioactive materials with the development of materials science and chemical science will shift to the field of creating more advanced biomaterials that could react or facilitate the implementation of various reactions with the biological environment depending on the state of the surface of the implanting material.

Without overlooking of the comparative analysis of the properties, advantages and disadvantages of artificial materials (for instance, see Nischenko et al., 2010; Puz, 2014; Vasilev et al., 2010), used in modern implantation surgery, in particular, in endoprosthetics, we list only the types of most frequently used materials, which can be toxic (surrounding tissues die off on contact), bioinert (non-toxic, but biological inactive) and bioactive (non-toxic, fused with bone tissue): composite biomaterials, bioglass and bioceramics; alloys of titanium, zirconium and magnesium. We will investigate only some aspects of laser surface treatment of titanium implants in this paper.

2. Brief overview of the basic properties of titanium implants. Laser treatment of the surface of titanium implants

2.1. Basic properties of titanium implants

For the first time, the concept of the use of industrially pure titanium and its alloys as implants was put forwarded by Swedish therapist P.-I. Branemark and his scientific group (for instance, see Adell et al., 1981; Branemark et al., 1977; and [23]): from the experimental work carried out in 1952-1969 it is showed the phenomenon of in growth of a titanium structure into living bone tissue (now this phenomenon is called osseointegration), and between the implant surface. The fibrous tissue does not form a fibrous or cartilaginous tissue. Since 1965, titanium implants have been used as bio- and mechanically compatible material for the manufacture of implants. Nowadays, numerous fundamental and clinical studies in vitro and in vivo have shown that industrially pure titanium, titanium-aluminum alloy, titanium-vanadium alloy, and nickel-titanium alloy having shape memory effect have such exceptional qualities as high mechanical strength, low cycle fatigue, plastic, high biocompatibility and biotolerance, antiallergenicity and lack of toxicity, high corrosion resistance due to the formation on the surface of a passivating oxide layer, low thermal conductivity, small coefficient of linear expansion, relatively low specific gravity, the smallest difference between the moduli of elasticity and bone. All listed properties of titanium and its alloys are based on their microstructures. As shown in Wang, & Zraigat, 2010, in order to reduce the modulus of elasticity of industrially pure titanium, the most effective

alloying elements for the additive are niobium (Nb), zirconium (Zr), molybdenum (Mo), tantalum (Ta). Nowadays, in the production of implants, industrially pure titanium grades BT1-0 and BT1-00 are used (for instance, see [61], Vasilev et al., 2010) from so called "commercially pure" titanium grades Ti-6Al-4V, Ti-6Al-7Nb; BT6, Grade-1 ÷ Grade-4, Grade-2H, Grade-6, Grade-7, Grade-7H, Grade-9, Grade-11 ÷ Grade-16, Grade-16H, Grade-17 ÷ Grade-26, Grade-26H, Grade-27 ÷ Grade-38.

It should be noted in conclusion that despite the very high mechanical properties of titanium alloys containing aluminum (Al) and vanadium (V), one should clearly know and distinguish the field of their application, because these elements can accumulate in the human body tissues and, due to the corrosive effect of biological fluids, cause acute allergies and have toxic effects. It is important to note that titanium implants, in spite of the above unique properties and advantages, still:

- undergo abrasive wear, which often leads to loss of the implant;
- can cause intolerable pain and pathogenicity due to the fact that wear products are deposited on the human body tissues.

Therefore, the unresolved and actual problem is the improvement of existing and development of new methods and technologies for the production of titanium implants and the treatment of their surfaces in order to enhance osseointegration contact, as well as proper biomechanical, chemical-biological (cell-matrix and nanoscale Level) of contacts between the implant and living human bone tissue.

2.2. Relevance and status of the issue

The state of the surface of titanium implants plays a decisive role in cell-cell adhesion. The interaction between the biological environment (hard and soft tissues, blood, body fluids and serum, etc.) and the implant occurs on its surface, and the biological response from the living tissue depends on a variety of surface properties, such as chemical composition, purity, texture and topography, surface energy, corrosion resistance, and the tendency to denaturalization of surrounding proteins. Nowadays, various methods of surface treatment of titanium implants to improve their biocompatible properties and to accelerate the healing process of implants are developed. These methods are based on morphological or biochemical modification of physical, chemical and mechanical properties, in particular, changes in surface energy and surface charge, chemical composition and surface printing of titanium implants. Approximately 20 years ago a new perspective direction arose related to the use of laser technology for surface treatment of biocompatible metallic materials, in particular titanium implants, in order to improve the tribological, biocompatible and corrosive properties of their surfaces. Theoretically, laser processing technology can possibly solve all the above tasks of modifying the complex of surface properties of titanium implants. Application of laser processing technology provides high spatial resolution and high processing speed, and does not affect the bulk properties of the processed material. Recent works (for instance, see Traini et al., 2017; Trisi et al., 2016; Vasilev et al., 2015 and appropriate references given in these) show that laser treatment of implant surfaces from titanium leads to the formation of a developed surface morphology characterized by a cellular structure, an increase in roughness and the formation of an inert oxide layer, which is necessary for improving the biocompatibility of titanium implants, in particular, enhancing the adhesion of living cells of different scales. In subsection conclusion, in the context of discussing the laser treatment advantages of

implant surfaces, let us dwell only on the results of the work Trisi et al., 2016: a group of Italian scientists carried out a rather curious experiment with the aim of:

- studying histomorphometric and biomechanical characteristics (BIC-bone-implant contact; RTV – reverse torque value) of titanium implants, which underwent laser treatment;
- comparing the ability of laser irradiation to stimulate osseointegration with a similar ability of titanium implants that have been mechanically processed.

The results of the experiment showed that RTV for titanium implants treated with a laser was almost 3 times higher than for those that received mechanical treatment; BIC titanium implants treated with a laser proved to be at least 30% better than BIC titanium implants, machined.

2.3. Describing the transfer of laser radiation during surface treatment of the titanium head of the endoprosthesis in terms of spherical trigonometry

Medical practice, especially in countries formerly part of the USSR, shows that repeated prosthetics of the hip joint of a person is associated with big problems (including due to the relatively high cost of surgery, inaccessible to many needy patients). In many cases, the implementation of such surgical operations becomes virtually impossible and, therefore, the life of the hip endoprosthesis is extremely important for the patient, especially at a young age. Modern joint endoprosthesis consists of an acetabular cup, a polyethylene liner; an endoprosthesis stem and a ball-shaped head (see Fig. 1). Titanium heads of the human hip joint endoprosthesis, in terms of the nature and magnitude of their load, are in extreme conditions (Novikov et al., 2011; Turmanidze et al., 2015), and therefore, the problem of improving the accuracy and quality of processing the most significant part of the endoprosthesis - the spherical surface of the head – is one of the most actual problems in modern endoprosthetics. Completely modern equipment for laser processing of materials, which has a Laboratory of Nanomaterials at the Institute of Basic Sciences and Innovative Technologies of the University of Liepaja (Nanomaterials Laboratory under the Institute of Fundamental Science and Innovative Technologies, Liepaja University), has a fixed head-source of laser radiation.

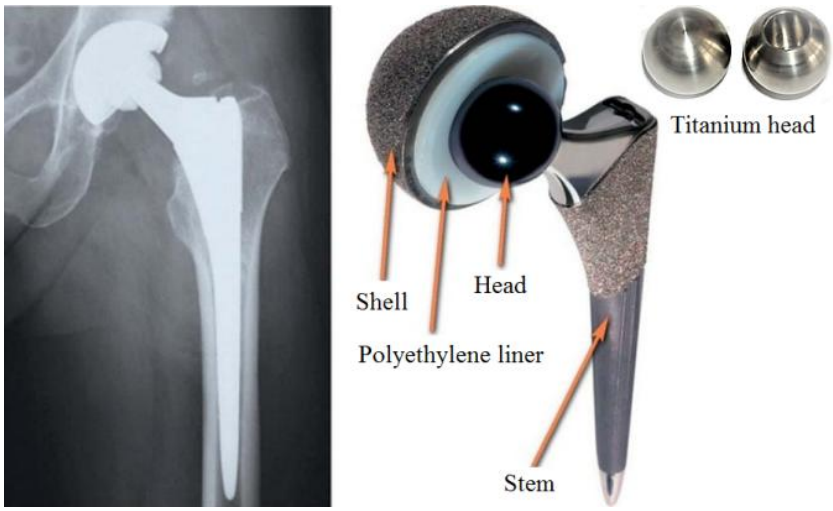

Fig. 1. Main components of a hip joint endoprosthesis.

Therefore, in order to carry out a high-precision uniform laser treatment, the endoprosthesis head, (which has a surface with a 270°-angle of the spherical segment) (see Fig. 2, Turmanidze et al., 2015), it is necessary to rotate the endoprosthesis head properly: the endoprosthesis head is fixed with a special holder in the vacuum chamber laser equipment, and this device can rotate the head of the endoprosthesis along two perpendicular axes with constant cycles per unit time (for each rotation axis its constant cycle).

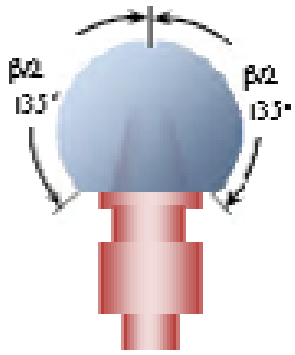

Fig. 2. The head of the endoprosthesis, which has a surface of β=270°-angle of the spherical segment

If the 3D laser-imaged material were a polyhedron, then the necessary calculation formulas for high precision and high-quality laser processing of this polyhedron can be derived from the corresponding mathematical model constructed in the Cartesian coordinate system. Obviously, because of the fact that: (a) the source of laser radiation on the existing laser equipment is stationary; (b) the endoprosthesis head has a spherical surface with a 270°-angle of the spherical segment being treated; (c) a two-coordinate holder can rotate the endoprosthesis head only in cycles, it is necessary to conduct studies using spherical trigonometry (for instance, see Palmer& Leigh, 1934; Ventsel, 1934): as the initial construction of the required adequate mathematical model in the Cartesian coordinate system with the subsequent derivation of the necessary calculation formulas obtained from it, and the "mechanical" translation of the equations and conditions of the already constructed mathematical model, as well as the resulting computational formulas from the Cartesian coordinate system to the spherical coordinate system, will not provide correct description of the process of precise, uniform and qualitative treatment of the spherical surface of the head of the endoprosthesis of the human hip joint. Indeed, in such a case, the work of the impact or (i.e. emitting laser radiation) is performed using the Euclidean metric as a measure of closeness between two points (a priori defined in the 3D Cartesian coordinate system), and the work of the affected object (i.e. reception of laser radiation on the spherical surface of the rotating head of the endoprosthesis) is carried out using a spherical metric as a measure of closeness between two points a priori defined in a 3D spherical coordinate system.

Consider the problem of transferring laser radiation in a parallel vertically inhomogeneous layer of a 3D spherical region (Fig.2), and, for simplicity, assuming the radius equal to 1. We make the following assumptions:

Assumption A. On the top border $z=0$ of analyzed layer with width of H and angle $\alpha_0=\arccos(\mu_0)$ falls laser power F laser irradiation in azimuthal plane β_0, $s_0=\{\alpha_0,\beta_0\}$.

Assumption B. Inside the layer under consideration and at its boundaries there may be diffusion sources of radiation.

Assumption C. The underlying surface at the lower boundary of the layer under consideration reflects the entire irradiation within a given law;

Assumption D. Transfer of irradiation occurs without changing the frequency.

The problem consists in determining the intensity of the multiply incident laser radiation inside the layer $0\le z\le H$, and also in determining the law of the reflected and missed laser radiation. As was mentioned above, the direction of propagation of multiple laser radiation at an arbitrary point of the layer $0\le z\le H$ It is necessary to describe with spherical coordinates: azimuth $\varphi=\frac{2}{5}\cdot(4\cdot\beta-\pi)\in[0,2\cdot\pi]$, where $\beta\in\left[\frac{\pi}{4},\frac{3\cdot\pi}{2}\right]$ characterizes the corresponding azimuth angle for the spherical segment of Fig. 2, and the zenith angle $\alpha\in[0,\pi]$, measured from the direction of the inner normal to the plane $z=0$ with unit vector $\vec{n}_0$, on OZ. In this case, as $\varphi=0$ accept the azimuth of the external laser beam $\beta_0=0$. Then direction $0^\circ\le\alpha=\alpha^+<90^\circ$ will be according the descending / missed radiation, and the direction $90^\circ<\alpha=\alpha^-\le180^\circ$ will correspond to the ascending / reflected radiation. We denote by: $\mu=\cos(\alpha)$, $\mu^+=\cos(\alpha^+)\in(0,1]$, $\mu^-=\cos(\alpha^-)\in[-1,0)$. Then the sets D^+ and D^-, are defined as

$D^+=\{(\mu,\varphi):\mu\in[0,1],\varphi\in[0,2\cdot\pi]\}$; $D^-=\{(\mu,\varphi):\mu\in[-1,0],\varphi\in[0,2\cdot\pi]\}$, will characterize the hemispheres of the directions of the descending / missed and ascending / reflected radiations. In this case, obviously, the set $D=D^+\bigcup D^-$ is a single sphere of directions for the transfer of laser radiation. If we denote the required intensity of the multiply-incident laser radiation inside the layer $0\le z\le H$ in direction $s=\{\alpha,\varphi\}$ through $I_{RI}(z,\mu,\varphi)$, so it can be written:

$$\mu\cdot\frac{\partial I_{RI}(z,\mu,\varphi)}{\partial z}+\left(f_t(z)+f_a(z)\right)\cdot I_{RI}(z,\mu,\varphi)=F(z,\mu,\varphi)$$
$$+f_r(z)\cdot\int_D I_{RI}(z,\tilde{\mu},\tilde{\varphi})\cdot\rho(z,\omega)\,d\tilde{\mu}d\tilde{\varphi}, \tag{1}$$

$$I_{RI}(z,\mu,\varphi)\big|_{\partial D_0}=g_0(\mu,\varphi)+F(0,\mu,\varphi)\cdot\delta(s-s_0), \tag{2}$$

$$I_{RI}(z,\mu,\varphi)\big|_{\partial D_H}=g_H(\mu,\varphi)+\frac{a\cdot\mu^2}{2\cdot\pi}\cdot\int_{D^+}\tilde{\mu}\cdot I_{RI}(H,\tilde{\mu},\tilde{\varphi})\,d\tilde{\mu}d\tilde{\varphi}, \tag{3}$$

where:

- function $f_t(z)$ and $f_a(z)$, through which the transmission and absorption coefficients of the laser radiation are designated, respectively, mean the physical characteristics of the surface of the endoprosthesis head;

– $\omega = \cos(\gamma)$, $\int_D \rho(s,\tilde{s})\,d\tilde{s} = 1$, $\int_D \rho(\omega)\,d\tilde{s} = 1$, $\int_{-1}^{+1} \rho(\omega)\,d\omega = \frac{1}{2\cdot\pi}$, where the transfer angle γ from direction $\tilde{s} = \{\tilde{\mu},\tilde{\varphi}\}$ in direction $s = \{\mu,\varphi\}$ is defined by the equation $\gamma = \arccos\left(\mu\cdot\tilde{\mu} + \sin(\alpha)\cdot\sin(\tilde{\alpha})\cdot\cos(\varphi-\tilde{\varphi})\right)$;
– in geometries $\{z,\alpha,\varphi\}$ and $\{z,\alpha\}$ boundary conditions (2) are determined on the following sets, respectively: $\partial D_0 = \left\{(z,\mu,\varphi):\ z=0,\ s\in D^+\right\}$, $\partial D_0 = \left\{(z,\mu):\ z=0,\ \mu\in(0,1]\right\}$;
– in geometries $\{z,\alpha,\varphi\}$ and $\{z,\alpha\}$ boundary conditions (3) are determined on the following sets, respectively: $\partial D_H = \left\{(z,\mu,\varphi):\ z=H,\ s\in D^-\right\}$, $\partial D_H = \left\{(z,\mu):\ z=H,\ \mu\in(-1,0]\right\}$.

As in the boundary conditions (3) the required function-intensity itself is present, then the proposed mathematical model (1)-(3) is a specific type of inverse boundary value problem for determining the function $I_{RI}(z,\mu,\varphi)$ in spherical geometry field $\{z,\mu,\varphi\} = [0,H]\times[-1,+1]\times[0,2\cdot\pi]$, in which all parameters defined in (1)-(3), but function $I_{RI}(z,\mu,\varphi)$, are assumed to be given, including the laws of the reflected and missed by the layer of laser radiation. We recall that in the complete formulation of the problem formulated above (see, after the enumerated assumptions A-D in this subsection), it was also required to determine the laws of the reflected and missed laser radiation. In the end, we would like to note that we can formulate two more mathematical models for determining, respectively, the law of reflected radiation and the law of laser radiation missed by the layer under consideration: both models have a more complex structure than model (1)-(3). In addition, it should be noted that the authors of this paper developed a numerical algorithm based on a combination of the Tikhonov regularization method (Tikhonov & Arsenin, 1977) and the method of characteristics (Delgado, 1997; Gelfand, 1959; Sarra, 2003), which makes it possible to realize the mathematical model (1)-(3).

3. Theoretical basis of the hydrophobic effect in a near-surface layer of several nanometers thick

3.1. Surface energy, surface tension and surface forces near the phase interfaces

Within representation of continuous medium, while analyzing two-phase systems, phase boundaries are interpreted as geometric surfaces. However, real phase boundaries are thin transition layers of a rather complicated structure. Molecules which form the transition layer interact with the molecules of both adjacent phases, that is why properties of transition layer differ from the properties of substance in the phases. This is the reason why during interpretation of phase boundaries there appear some phenomenological properties. Correct description of microsurface forces lies in the foundation of surface tension's and capillarity's interpretation both in the old approach of Clairaut and Laplace and in the new approach of Bakker (Bakker, 1928; Blkerman,

1978; Rusanov & Goodrich, 1980), which is based on introducing the pressure tensor in the interphase area. Description of microsurface forces should begin with definition of interphase energy on the surface of phase boundary of solid-liquid phases (and also phases of liquid-liquid, liquid-gas, solid-solid) and proceed with definition of surface forces in the interphase area. It is known (Churaev, 1987) that if both phases are fluid (liquid-liquid, liquid-gas), then their phase boundary can be stretched or shrank not affecting the thermodynamic equilibrium; if one phase is solid and the other is liquid or gaseous, then surface of their phase boundary can experience only elastic deformations, however some degree of freedom appears if the liquid is able to slide on the sufficiently smooth solid material (for example, like when quicksilver slides down the glass; water slides on the paraffin surface; blood or body fluids slide down the burnished surface of a titanium implant, etc.); if both phases are solid, then behavior of the phase boundary is similar to the case solid-liquid, however the implementation of a real phase contact is possible only with atomic smoothness or requires plastic deformation, or prior melting, or evaporation and condensation with subsequent crystallization. Only in the case, when both phases are fluid, direct measurement of phase boundary tension is possible. In the case, when both phases are solid, direct measurement of phase boundary tension is achievable with some approximation if and only if in some temperature region yield point is lowered. In the case, when one phase is solid and the other is gaseous, direct measurement of phase boundary tension is impossible. The main mistakes made while measuring surface energy in the process of formation of a new surface are:

- omission of irreversible part of fracture work, which turns into heat or energy residual deformations;
- omission of the fact that fresh (that is, just created) surfaces are in nonequilibrium state with higher energy – they appear to be covered by charge with density up to $3.5 \cdot 10^{-4}\, C \cdot m^{-2}$, that consumes part of the fracture work.

The special state of fresh surfaces is expressed not only by increased energy, but also by a higher chemical activity. Relaxation down to equilibrium state usually occurs for about ten minutes due to electron emission and surface conduction. Formation of a new phase boundary is conjugate with consumption of work in order to move a part of molecules from the phases to the surface layer. In isothermal conditions the work of formation of phase surface's element dF is equal to increment of Helmholtz energy dU_F of the surface: $dU_F = \sigma \cdot dF$, where σ is specific Helmholtz energy of the phase boundary, which decreases as the temperature increases and at critical temperature $T_{c.t.}$ achieves the approximate value of zero (in steam-and-liquid systems $\sigma = 0$, and the difference between the phases disappears). The values of σ for the surface of a solid body on a border with a liquid are not identical to the corresponding coefficients of surface tension (Gokhshtain, 1976). Accurate theoretical formulas for calculation of liquids' surface tension coefficient do not exist. The main methodological difficulty of calculation of surface tension is the problem of ensuring solid surface purity, when it is in contact with a liquid, as well as liquid's purity. There are some methods of experimental calculation among which the most popular are (Kikoin & Kikoin, 1976): maximum gas bubble pressure method*; capillary rise method;* method of ring lifting; electromagnetic measurement methods; the drop weight method; hanging drop method; lying bubble or drop method. The simplest experimental method of determining the empirical dependence of phase boundary's specific Helmholtz energy on the temperature is the following relation obtained from the theory of corresponding states

([47]): $\sigma = \sigma_0 \cdot \left(1 - \frac{T}{T_{c.t.}}\right)^{\frac{11}{9}}$, where σ_0 is determined by the experiments carried out with one constant value of temperature. This formula has shown itself well working for liquids with homonuclear molecules; however it can be approximately used also for the majority of other liquids. For calculations of water's σ it is recommended to use the following interpolation formula: $\sigma = 0.235 \cdot \left(1 - \frac{T}{T_{c.t.}}\right)^{1.256} \cdot \left(1 - 0.625 \cdot \frac{T_{c.t.} - T}{T_{c.t.}}\right)$.

3.2. Wetting process

In the introduction we mentioned (following the work Adamson & Gast, 1997 the contact angle of wetting θ between a solid surface and a tangent to the phase boundary gas-liquid. From the minimality condition of surface's Helmholtz energy (Kikoin & Kikoin, 1976; Labuntsov & Yagov, 1977; Landau & Lifshitz, 1987) one can obtain the following relation known as Young's law: $\theta = \text{arccosine}\left(\frac{\sigma_{solid,gas} - \sigma_{solid,liquid}}{\sigma}\right)$. It is important to note that the contact angle is very sensitive to such difficult-to-control factors as roughness of a solid surface or presence of foreign impurity on the solid surface or in the liquid, particularly if this impurity is surface-active, which, concentrating on the thermodynamic phase boundary, cause surface tension lowering: for instance, R-OH alcohols; R-COH aldehydes; R-COOH carboxylic acids; CH3-, C2H5-, C17H35-, etc. hydrocarbon radicals; COH and COOH functional groups; oleic acid C17H33COOH; stearic acid sodium C17H35COONa; etc. Rise in the roughness of the solid surface increases its wettability, that is, decreases the value of θ. For some solid bodies participating in the phase solid-liquid in a certain interval of temperature holds a dependence of the contact angle θ on the temperature (Zimon, 1974). As it is shown in Zimon, 1974, almost always a growth of temperature on a hydrophilic surface leads to improvement of wettability, that is, to diminution of the angle θ, but on hydrophobic surfaces – to worsening of wettability, that is, to growth of the angle θ. Also it is important to note (especially, if we are speaking about implants) that the contact angle of wetting θ depends also on hysteresis of wetting – on the direction of wetting a solid body surface by a liquid, that is, on the fact, whether the liquid is flowing on the surface or down it.

3.3. The phase separation surface's equilibrium and axisymmetric equilibrium separation surfaces of phases

If the liquid rests relative to the coordinate system related to Earth, then in hydromechanics this rest is called absolute rest; if the liquid rests relative to the coordinate system which moves with uniform acceleration relative to Earth, then this rest is called relative rest. For both absolute rest and relative rest Euler's equations in the vector form hold: $\vec{F} - \frac{1}{\rho} \cdot \nabla p = 0$, where $\vec{F}$ is mass forces density vector, which, in the case of relative rest, includes inertial forces; ρ is liquid density; p is liquid pressure. Due to the fact that mass forces have potential in the majority of cases, one can write

$\vec{F} = -\nabla\Phi$, where Φ is a force function. Consequently, the Euler's equation turns into equation $\nabla\Phi + \frac{1}{\rho}\cdot\nabla p = 0$, whose general integral for the cases, when $\rho = \rho(p)$, is the formula $\Phi + \Upsilon = const$, called the equation of hydrostatics, where $\Upsilon = \int \frac{dp}{\rho}$ denotes pressure function. It should be noted that, if the liquid is a heavy compressible liquid, then out of all mass forces only gravitational force affects it, so the general integral looks like $\Phi = g\cdot z + const$, where z denotes the coordinate which is counted vertically up. For a heavy compressible liquid the general integral of Euler's equation has the form $z + \frac{p}{g\cdot\rho} = const$, and this formula represents hydrostatic distribution of pressure. When a gas-liquid system is in the equilibrium state, then in each contacting phase, firstly, the equations of hydrostatics hold and, secondly, for every point on phase boundary defined by a position vector $\vec{r}$ Laplace formula $p_1 - p_2 = 2\cdot\sigma\cdot H(\vec{r})$ is true, which means that on the boundary between two fluid phases the surface tension causes a pressure jump in the contacting phases, which is proportional to average curvature H of the phase boundary. From these two relations (equation of hydrostatics and Laplace formula) one can deduce the main differential equation of hydrostatic equilibrium, whose general integral $2\cdot\sigma\cdot H(\vec{r}) = (\rho_{liquid} - \rho_{gas})\cdot\Phi(\vec{r}) + const$ determines the shape of phase boundary. In the most practically important axial-symmetric problems on liquid there are: homogeneous gravitational field with intensity g, directed along vertical axis OZ; centrifugal force field caused by uniform rotation of the gas-liquid system around the same axis OZ with angular velocity ω. In this case, the potential of mass forces has the form $\Phi = g\cdot z - \frac{1}{2}\cdot\omega^2\cdot d^2$, where $d = \sqrt{x^2 + y^2}$ is the distance to the rotation axis. When the system rests, potential of mass forces is determined by the formula $\Phi = g\cdot z$, but the main equation of hydrostatic equilibrium has the form: $2\cdot\sigma\cdot H(z) = \delta\cdot g\cdot(\rho_{liquid} - \rho_{gas})\cdot z + 2\cdot\sigma\cdot H(0)$, where the term $2\cdot\sigma\cdot H(0)$ represents the pressure jump on some "zero" level; $\delta = +1$ in the case, when the vertical axis OZ is pointed up (and the gravitational field is pointed down), and $\delta = -1$ in the case, when the vertical axis OZ is pointed down. For a resting system with a characteristic size $L_{ch.d.}$ it is possible to use the main equation of hydrostatic equilibrium in order to obtain the scale of gravitational forces $f_{grav} \sim g\cdot(\rho_{liquid} - \rho_{gas})\cdot L_{ch.d.}$ and the scale of surface tension forces $f_{s.t.} \sim \frac{\sigma}{L_{ch.d.}}\cdot$ Then Bond number Bo, which is the criterion of similarity in hydrodynamics and determines relation between external forces (usually, gravity) and surface tension forces has the following form: $Bo = \frac{f_{grav}}{f_{s.t.}} = g\cdot(\rho_{liquid} - \rho_{gas})\cdot\frac{L^2_{ch.d.}}{\sigma}$. The condition $Bo = 1$ determines linear size of the region, where gravitational forces and surface tension forces are equal: $L_{lin.d.} = \sqrt{\frac{\sigma}{g\cdot(\rho_{liquid} - \rho_{gas})}}$. The quantity $L_{lin.d.}$ is called

capillary constant. For the majority of liquids with $p \ll p_{c.t.}$ ($p_{c.t.}$ is critical pressure), that is, in Earth conditions, the value of capillary constant varies within $1 \div 3$ *mm.* Obviously, if one divides the equation of hydrostatic equilibrium $2 \cdot \sigma \cdot H(z) = \delta \cdot g \cdot (\rho_{liquid} - \rho_{gas}) \cdot z + 2 \cdot \sigma \cdot H(0)$ by the quantity $\sqrt{\sigma \cdot g \cdot (\rho_{liquid} - \rho_{gas})}$, then it turns into the following dimensionless form: $2 \cdot \tilde{H}(\tilde{z}) = \delta \cdot \tilde{z} + C$, where $\tilde{H} = L_{lin.d.} \cdot H$, $\tilde{z} = \dfrac{z}{L_{lin.d.}}$, $C = 2 \cdot H(0) \cdot L_{lin.d.}$.

3.4. Melting, deformation and crystallization processes

At sufficient energy density, duration and order of a laser pulse melting of solid body's surface occurs – in our case, of ball-shaped titanium head of the human hip joint endoprosthesis. When the laser pulse irradiation stops, the process of cooling the processed surface starts and is carried out by the means of heat removal deep into the solid phase and subsequent solidification of the surface layer. It is supposed that the power of laser irradiation is such that phase transition solid-liquid occurs. Then, with appropriate approximation, temperature fields in the liquid $T_{liquid}(x,t)$ and solid $T_{solid}(x,t)$ phases can be described by following boundary value problem (Kendall, 1994; Khasaya et al., 2014; Mikolutskiy et al., 2013):

$$\frac{\partial T_{liquid}(x,t)}{\partial t} = a_{liquid} \cdot \frac{\partial^2 T_{liquid}(x,t)}{\partial x^2}, \; 0 < x < y(t), \tag{4}$$

$$\frac{\partial T_{solid}(x,t)}{\partial t} = a_{solid} \cdot \frac{\partial^2 T_{solid}(x,t)}{\partial x^2}, \; y(t) < x < \infty, \tag{5}$$

$$T_{solid}(x,t)\big|_{t=0} = T_{solid}(x,t)\big|_{x=\infty} = T_0, \tag{6}$$

$$\frac{\partial Q(t)}{\partial t} + \lambda_{liquid} \cdot \frac{\partial T_{liquid}(x,t)}{\partial x}\bigg|_{x=0} = 0, \tag{7}$$

$$T_{liquid}(x,t)\big|_{x=y(t)} = T_{solid}(x,t)\big|_{x=y(t)} = T_1, \tag{8}$$

$$\lambda_{liquid} \cdot \frac{\partial T_{liquid}(x,t)}{\partial x}\bigg|_{x=y(t)} = H \cdot \rho \cdot y'(t) + \lambda_{solid} \cdot \frac{\partial T_{solid}(x,t)}{\partial x}\bigg|_{x=y(t)}. \tag{9}$$

Here $y(t)$ is the moving boundary of the phase transition; $Q(t)$ is the absorbed energy per surface unit for the time $t \ll \tau$, here τ denotes the duration of a laser pulse; $a = \dfrac{\lambda}{c \cdot \rho}$ is a thermal diffusivity, where λ, c and ρ denote correspondingly thermal conductivity, specific heat and density of a metal $(a_{solid}, \lambda_{solid}, c_{solid}, \rho_{solid})$ or liquid $(a_{liquid}, \lambda_{liquid}, c_{liquid}, \rho_{liquid})$; T_0 and T_1 denote correspondingly initial temperature of the solid body and the temperature of the phase transition; H is a latent melting heat, which is absorbed on the moving phase boundary. Supposing that the temperature of the metal surface processed by laser pulse achieves phase transition point during the time $t_0 \ll \tau$

and the temperature of liquid phase varies slightly during further process $t_0 < t < \tau$, we can replace the boundary condition (4) by the following more simple condition:

$$T_{liquid}\left(x,t\right)\Big|_{x=0} = T_2 = T_{liquid}\left(x,\tau\right)\Big|_{x=0} > T_1, \tag{10}$$

where T_2 is a temperature of molten metal on the surface that can be defined by heat balance equation.

Combining (4)-(6), (8) and (10) we can write that

$$T_2 = T_1 + \frac{erf\left(\dfrac{\beta}{\sqrt{2\cdot a_{liquid}}}\right)}{2\cdot c_{liquid}\cdot\rho\cdot\sqrt{a_{liquid}}\cdot\left(1-e^{-\frac{\beta^2}{2\cdot a_{liquid}}}\right)\cdot erfc\left(\dfrac{\beta}{\sqrt{2\cdot a_{solid}}}\right)}\times$$
$$\times\left\{\left(\sqrt{\frac{\pi}{\tau}}\cdot Q\left(\tau\right)-\sqrt{2\cdot\pi}\cdot H\cdot\rho_{solid}\cdot\beta\right)\cdot erfc\left(\frac{\beta}{\sqrt{2\cdot a_{solid}}}\right)-2\cdot c_{solid}\cdot\rho_{solid}\cdot\left(T_1-T_0\right)\right\}, \tag{11}$$

where $erf\left(\omega\right)=\dfrac{2}{\sqrt{\pi}}\cdot\int\limits_0^{\omega}e^{-\xi^2}d\xi$ is the Gauss error function; $erfc\left(\omega\right)=1-erf\left(\omega\right)$ is the complementary error function; the parameter β can be found from the following transcendental equation:

$$\frac{2\cdot\sqrt{\dfrac{a}{\pi}}c\cdot\rho\cdot\left(T_1-T_0\right)}{erfc\left(\dfrac{\beta}{\sqrt{2\cdot a}}\right)}=\sqrt{2}\cdot H\cdot\rho\cdot\beta\cdot\left(e^{-\frac{\beta^2}{2\cdot a}}-2\right)+\frac{Q\left(\tau\right)}{\tau}, \tag{12}$$

$$Q\left(\tau\right)=H\cdot\rho\cdot y\left(\tau\right)+\int\limits_0^{y(\tau)}c_{solid}\cdot\rho_{solid}\cdot\left(T_1-T_0\right)dx+\int\limits_0^{y(\tau)}c_{liquid}\cdot\rho\cdot\left(T_{liquid}-T_1\right)dx$$
$$+\int\limits_{y(\tau)}^{\infty}c_{solid}\cdot\rho_{solid}\cdot\left(T_{solid}-T_0\right)dx. \tag{13}$$

The formulas (11)-(13) allow us to calculate melting depth of different solid materials irradiated by laser pulses of various duration and energy. As it has already been mentioned above, under the influence of laser irradiation high temperature stress occurs in the metals. Deformation process in these conditions is followed by residual deformation, whose appearance is related to nonelastic effects and reorganization of crystal's defect structure. Stress' relaxation can have heterogeneous character due to formation of new structure zones called relaxation zones (Khomich et al., 2012) in the old excited structure. Depending on the state of the system, on the conditions of external influence, on the degree of process development it may occur that relaxation zones can be centers of a new phase, groups of dislocations and disclinations, microcracks, clusters of atoms and vacancies forming clusters, micropore, dislocation loops, etc. One can imagine the deforming as three simultaneously coexistent phases: relaxation field determined by the parameter $\varphi_{i,j}\left(r,t\right)$, stress field $\sigma_{i,j}\left(r,t\right)$ corresponding to external load and relaxation zones with concentration $n\left(r,t\right)$. Temporary dependence $\varphi_{i,j}\left(r,t\right)$,

$\sigma_{i,j}(r,t)$ and $n(r,t)$ is defined by the following system of nonlinear differential equations:

$$\begin{cases} \dot{\varphi}_{i,j} = -\kappa \cdot \varphi_{i,j} + g_1 \cdot n; \\ \dot{n} = -\gamma \cdot n + \dfrac{\varphi_{i,j} \cdot \sigma_{i,j}}{g_2}; \\ \dot{\sigma}_{i,j} = \nu \cdot \left(\sigma_{i,k} - \sigma_0\right) - g_3 \cdot \varphi_{i,j} \cdot n, \end{cases} \tag{14}$$

where parameters κ, γ, ν, g_i $\left(i = \overline{1,3}\right)$ are material constant; quantity σ_0 is determined by the applied external loads and corresponds to the residual stress set as the result of relaxation.

In the system (14) the term $-\kappa \cdot \varphi_{i,k}$ is the decay of the relaxation process; the term $-\gamma \cdot n$ describes disintegration of the formed relaxation zones; the term $\nu \cdot \left(\sigma_{i,k} - \sigma_0\right)$ describes the stress relaxation in linear approximation, when their interference is absent; the term $g_1 \cdot n$ is related to relaxation field generation due to formation of relaxation zones; the term $\dfrac{\varphi_{i,k} \cdot \sigma_{i,k}}{g_2}$ takes into account the influence of the relaxation field $\varphi_{i,j}(r,t)$ and stress field $\sigma_{i,j}(r,t)$ on the generation of relaxation zones; the term $g_3 \cdot \varphi_{i,j} \cdot n$ is caused by the influence of the relaxation field and relaxation zones on the speed of stress relaxation. As the speed of alteration of the relaxation field is much lower than the speed of the processes atomic relaxation described by the constants γ and ν, in (10) one can use adiabatic elimination of variables. Taking into account possible spatial fluctuations whose role grows as temperature and external loads grow, we get the following kinetic equation for relaxation parameter:

$$\varphi_{i,j} = D \cdot \Delta\varphi_{i,j} + \frac{g_1}{g_2 \cdot \gamma} \cdot \left\{ \left(\sigma_0 - \frac{g_2 \cdot \gamma}{g_1} \cdot \kappa \right) \cdot \varphi_{i,j} - \frac{g_3 \cdot \sigma_0}{g_2 \cdot \gamma \cdot \nu} \cdot \varphi_{i,j}^3 \right\}, \tag{15}$$

where D is a diffusion coefficient of atoms in a warmed-up zone.

If we take into account diffusion's dispersion, then equation (15) will turn into the well-known Ginzburg-Landau generalized equation (Gurtin, 1996; Hohenberg & Krekhov, 2015). For $\sigma_0 < \sigma_c = \dfrac{g_2 \cdot \gamma}{g_1} \cdot \kappa$ equation (15) has one stable solution $\varphi_{i,j}(r,t) = 0$; if exceeding of the critical value $\sigma_0 > \sigma_c$ occurs, new coherent states of the system are realized with spatial periodicity, whose period can be calculated using the formula $P = \dfrac{\sigma_0 - \sigma_c}{2 \cdot \pi \cdot \sigma_0} \cdot \sqrt{\dfrac{3 \cdot D}{8 \cdot \nu}}$. Using the kinetic equation from the theory of surface nucleation (see Adell et al., 1981; Barret, 1973; Deb, 2014; Pomogailo & Kestelman, 2005) as well as variational principle for the main laws of thermal conduction, one can obtain (Tokarev et al., 2010) the following closed formula for characteristic size-radius of a crystalline phase nucleus in a supercooled liquid:

$$r(t) = \nu_0 \cdot d \cdot e^{-\frac{U}{k \cdot T_1}} \cdot \frac{k \cdot T_1^2}{U \cdot \varepsilon} \cdot \left(\frac{h}{U+h} - e^{-\frac{U \cdot \varepsilon \cdot t}{k \cdot T_1^2}} + \frac{U}{U+h} \cdot e^{-\frac{(U+h) \cdot \varepsilon \cdot t}{k \cdot T_1^2}} \right), \quad (16)$$

where ν_0 is Debye oscillation frequency of atoms in a supercooled liquid; U is the activation energy for atom movement; $k \cdot T$ is thermal energy; d is characteristic size for a single atom; h is the heat of phase transformation for one atom; ε is the average speed of melt cooling. Using the formula (16) one can precisely estimate characteristic size-radius of a crystalline phase nucleus, that is, the size of nanostructures appearing on the surface of the processing solid body, while it is melting under laser pulse irradiation.

4. Experimental facilities, experiments and obtained results

4.1. Experimental facilities

Within present work we have carried out two types of series of experiments. The first type of series consists of 6 experiments devoted to direct laser nanostructuring of titanium (Ti) surface curved into a geometric shape resembling a cylinder (see Fig. 3). The second type of series consists of 6 experiments devoted to direct laser nanostructuring of titanium (Ti) and copper (Cu) surfaces. All the processed samples had the same sizes: $L \times W \times H = 5 \times 3 \times 0.1\ mm.$ In the case of the first type of series of experiments, the height is understood as the thickness of the titanium sheet. Samples' surfaces had 14th surface finish class. Samples were placed in a laser facility chamber Nd^{3+}:YAG crystal and were irradiated in a motionless laser beam.

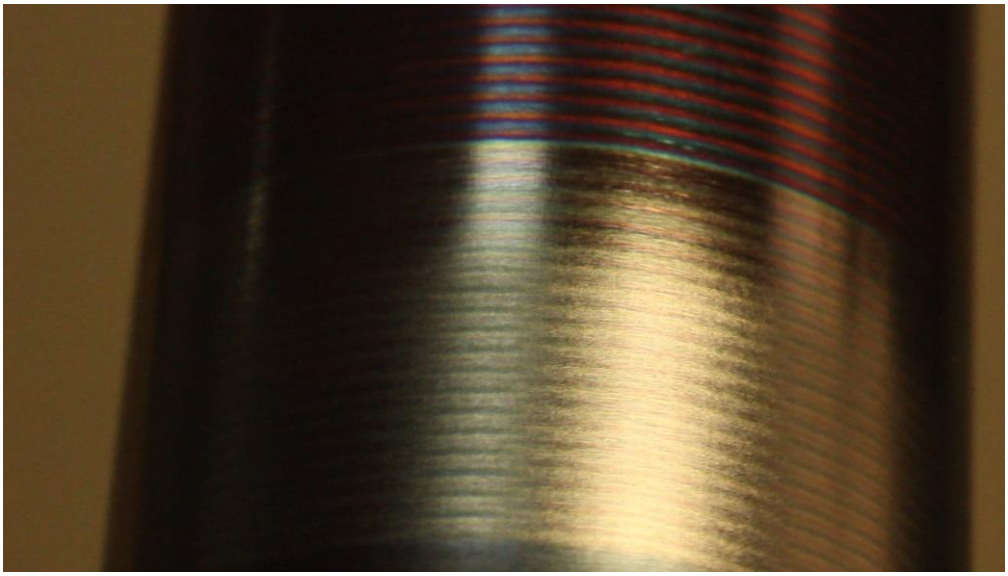

Fig.3. Titanium sheet curved into a geometric shape resembling a cylinder: the present picture is taken as a frame from the video filming of surface processing by a direct laser irradiation.

For a detailed analysis of the irradiated samples' profiles we use dadesktop scanning electron microscope TM3030 with low vacuum regime, which allows one to carry out the experiments without sample preparation and to investigate samples without prior metal deposition; controlled by a simple and understand able inter face with the functions of automatic focus, contrast and brightness setting; equipped with two detectors – of secondary and reflected electrons, – owing to which it is possible to

get comprehensive information about the surface of the investigated samples. Laser facility Nd^{3+}:YAG crystal, which was used in order to carry out a series of experiments devoted to direct laser nanostructuring of surfaces of 10 titanium samples (6 and 4 samples for the first and the second types of series, respectively) and 2 copper samples, has the following capabilities:

- laser wavelength: 532 nm;
- maximum pulse energy: 0.15 J;
- pulse repetition rate: 10 Hz;
- initial pulse duration: 5÷9 ns;
- pulse duration: 5÷400 μs.

After repeated irradiation with one beam of micro second Nd^{3+}:YAG crystal-laser formation of nano sized structures on the copper and titanium surfaces was noticed. Laser irradiation intensity was maximal in the center of the irradiation spot and was going down closer to its periphery. After repeated pulsation on one surface patch a deep crater appeared in the spot's center. However, on the periphery, where the laser irradiation intensity was lower, one could notice only some surface melting. Using SEM-analysis (that is, using scanning electron microscopy with X-ray spectrometry microanalysis) no sub micrometer structures were detected in the central high-intensity part of the spot. However, formation of nanorelief was detected in the peripheral part of the irradiation zone. For all 12 samples we detected roughness of characteristic size along the surface on the surface in the peripheral low-intensity region of the spot as well as small-scale roughness in the form of saliences put over the surface. Round shape of the obtained nanorelief simplies the surface being molten by the laser irradiation and subsequent crystallization with formation of the above mentioned submicrometer structures. Taking into account the possibility of slight material melting, we can consider a surface under thermal flow of pulsed laser irradiation which causes phase transition solid-liquid.

4.2. The first type of series of experiments by titanium sheet curved into a cylinder, and obtained results

Experiment I-1. In this experiment titanium surface was taken as a sample, and for its laser processing the following characteristics of microsecond laser facility Nd^{3+}:YAG crystal were chosen: laser wave length (LW): 532 nm; pulse energy (PE): 0.15 J; pulse repetition rate (PRR): 10 Hz; pulse duration (PD): 150 μs.

Results of a three foldpulse action on this sample are shown on the Fig. 4. The obtained nanostructured surface has a very good ultra-hydrophobicproperty with an average interfacial contact angle $\theta_{average} \approx 169°$, where distilled water was used as the liquid.

Experiment I-2. In this experiment titanium surface was taken as a sample, and for its laser processing the following characteristics of microsecond laser facility Nd^{3+}:YAG crystal were chosen:

- laser wavelength (LW): 532 nm;
- pulse energy (PE): 0.15 J;
- pulse repetition rate (PRR): 10 Hz;
- pulse duration (PD): 150 μs.

Results of a twofold pulse action on this sample are shown on the Fig. 5. The obtained nanostructured surface has an average quality of hydrophobicity with an

average interfacial contact angle $\theta_{average} \approx 124°$, where distilled water was used as the liquid also.

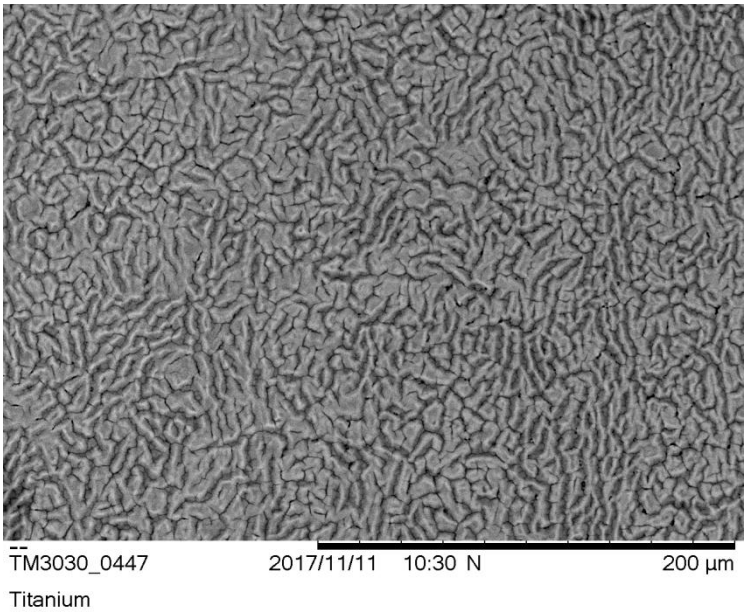

Fig 4. Nanostructured titanium surface (three-times processing; texture magnification: 500x) with an average contact angle of 169° (very good ultra-hydrophobic property). Nd3+:YAG crystal-laser's features: LW=532 nm; PE=0.15 J; PRR=10 Hz; PD=150 µs.

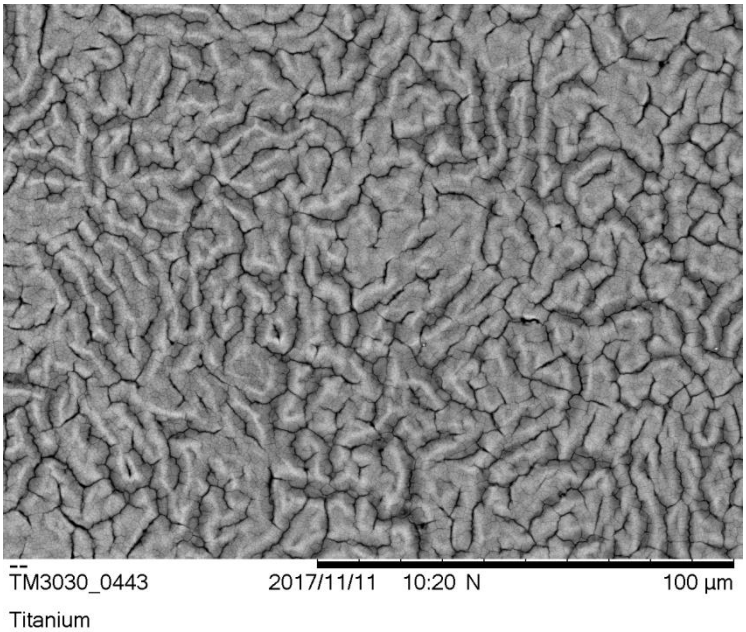

Fig. 5. Nanostructured titanium surface (two-times processing; texture magnification: 500x) with an average contact angle of 124° (average hydrophobic property). Nd3+:YAG crystal-laser's features: LW=532 nm; PE=0.15 J; PRR=10 Hz; PD=150 µs.

Experiment I-3. In this experiment titanium surface was taken as a sample, and for its laser processing the following characteristics of microsecond laser facility Nd^{3+}:YAG crystal were chosen:

– laser wavelength (LW): 532 nm;

– pulse energy (PE): 0.15 J;
– pulse repetition rate (PRR): 10 Hz;
– pulse duration (PD): 150 μs.

Results of a single pulse action on this sample are shown on the Fig. 6. The obtained nanostructured surface has an average quality of hydrophobicity with an average interfacial contact angle $\theta_{average} \approx 118°$, where water was used as the liquid.

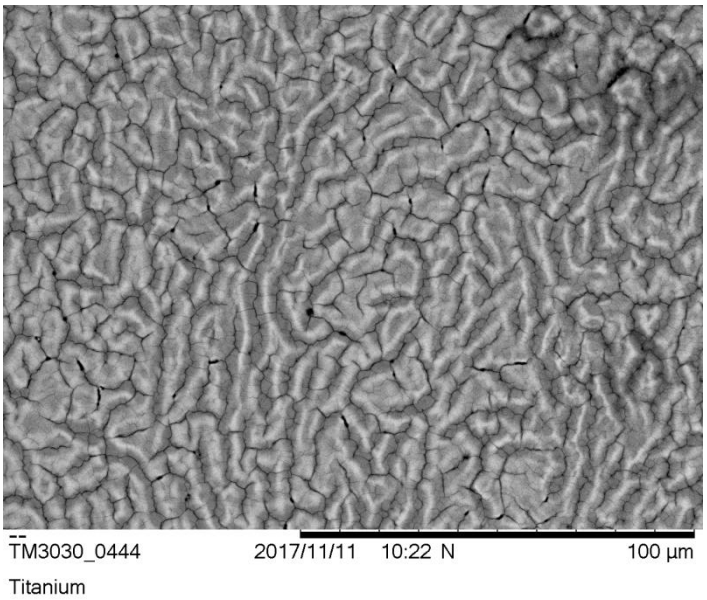

Fig 6. Nanostructured titanium surface (one-time processing; texture magnification: 1000x) with an average contact angle of 118° (average hydrophobic property). Nd3+:YAG crystal-laser's features: LW=532 nm; PE=0.15 J; PRR=10 Hz; PD=150 μs.

Experiment I-4. In this experiment titanium surface was taken as a sample, and for its laser processing the following characteristics of microsecond laser facility Nd^{3+}:YAG crystal were chosen:

– laser wavelength (LW): 532 nm;
– pulse energy (PE): 0.15 J;
– pulse repetition rate (PRR): 10 Hz;
– pulse duration (PD): 300 μs.

Results of a single pulse action on this sample are shown on the Fig. 7. The obtained nanostructured surface has alow-quality of hydrophobicity with an average interfacial contact angle $\theta_{average} \approx 97°$, where water was used as the liquid.

Experiment I-5. In this experiment titanium surface was taken as a sample, and for its laser processing the following characteristics of microsecond laser facility Nd^{3+}:YAG crystal were chosen:

– laser wavelength (LW): 532 nm;
– pulse energy (PE): 0.15 J;
– pulse repetition rate (PRR): 10 Hz;
– pulse duration (PD): 300 μs.

Results of a twofold pulse action on this sample are shown on the Fig. 8. The obtained nanostructured surface has a barely perceptible quality of hydrophobicity with an average interfacial contact angle $\theta_{average} \approx 90°$, where water was used as the liquid.

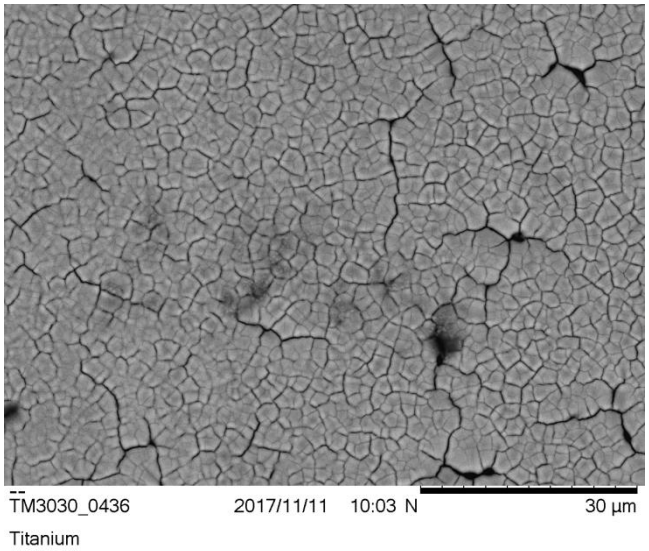

Fig.7. Nanostructured titanium surface (one-time processing; texture magnification: 2000x) with an average contact angle of 97° (slight shows of hydrophobic property). Nd3+:YAG crystal-laser's features: LW=532 nm; PE=0.15 J; PRR=10 Hz; PD=300 µs.

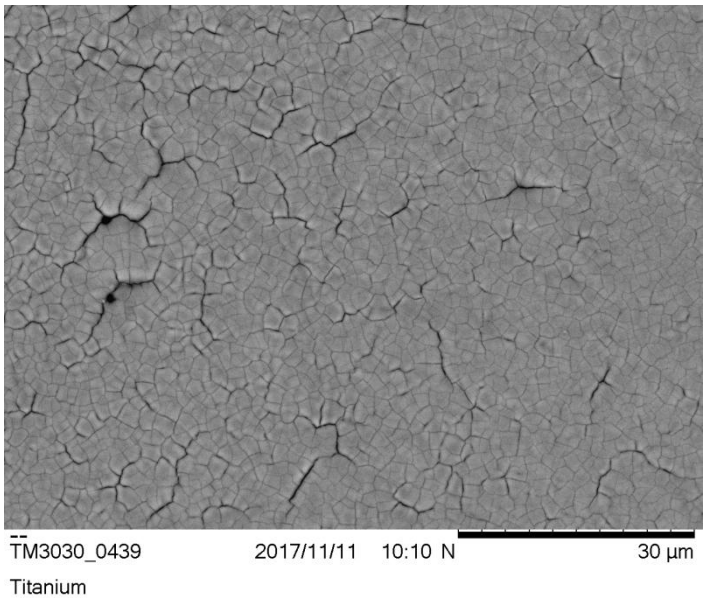

Fig. 8. Nanostructured titanium surface (two-times processing; texture magnification: 2000x) with an average contact angle of 90° (poor hydrophobic property). Nd3+:YAG crystal-laser's features: LW=532 nm; PE=0.15 J; PRR=10 Hz; PD=300 µs.

Experiment I-6. In this experiment titanium surface was taken as a sample, and for its laser processing the following characteristics of microsecond laser facility Nd^{3+}:YAG crystal were chosen:

- laser wave length (LW): 532 nm;
- pulse energy (PE): 0.15 J;
- pulse repetition rate (PRR): 10 Hz;
- pulse duration (PD): 300 µs.

Results of a threefold pulse action on this sample are shown on the Fig. 9. The obtained nanostructured surface has not hydrophobicity (and has poor hydrophilicity)

with an average interfacial contact angle $\theta_{average} \approx 84°$, where water was used as the liquid.

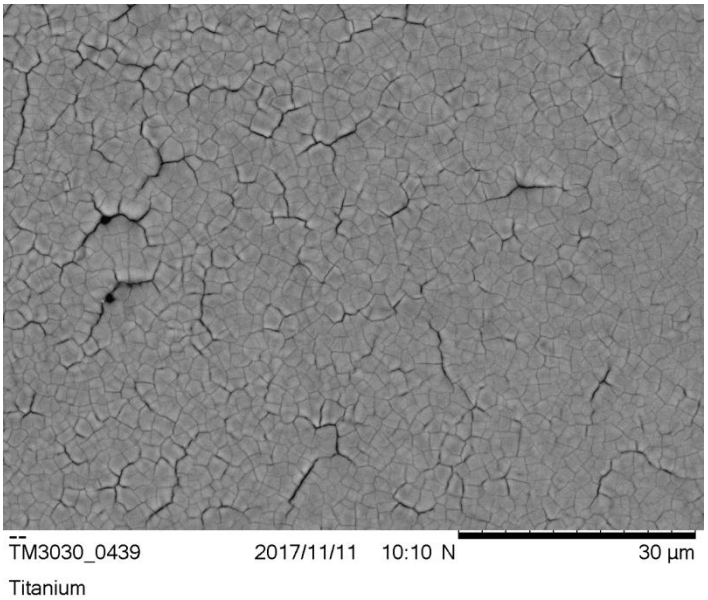

Fig. 9. Nanostructured titanium surface (three-times processing; texture magnification: 2500x) with an average contact angle of 84° (no hydrophobic property, and with poor hydrophilic property). Nd3+:YAG crystal-laser's features: LW=532 nm; PE=0.15 J; PRR=10 Hz; PD=300 µs.

4.3. The second type of series of experiments and obtained results

Experiment II-1. In this experiment copper foil was taken as a sample, and for its laser processing the following characteristics of microsecond laser facility Nd^{3+}:YAG crystal were chosen:

- laser wavelength (LW): 532 nm;
- pulse energy (PE): 0.14 J;
- pulse repetition rate (PRR): 10 Hz;
- pulse duration (PD): 130 µs.

Results of a single pulse action on this sample are shown on the Fig.10. The obtained nanostructured surface has a good hydrophilic property with an average interfacial contact angle $\theta_{average} \approx 51°$, where water was used as the liquid.

Experiment II-2. In this experiment copper foil was again taken as a sample, and for its laser processing the following characteristics of microsecond laser facility Nd^{3+}:YAG crystal were chosen:

- laser wavelength (LW): 532 nm;
- pulse energy (PE): 0.14 J;
- pulse repetition rate (PRR): 10 Hz;
- pulse duration (PD): 130 µs.

Results of a twofold pulse action on this sample are shown on the Fig. 11. The obtained nanostructured surface has a much worse hydrophilic property (more exactly, has hydrophobic property) with an average interfacial contact angle $\theta_{average} \approx 115°$, where a water was used as the liquid.

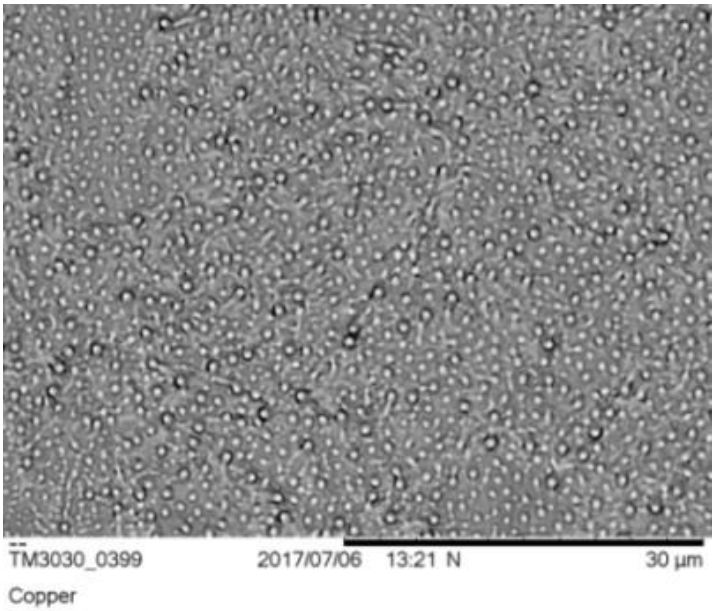

Fig. 10. Nanostructured copper surface (one-time processing) with an average contact angle of 51° (good hydrophilic property). Nd3+:YAG crystal-laser's features: LW=532 nm; PE=0.14 J; PRR=10 Hz; PD=130 µs.

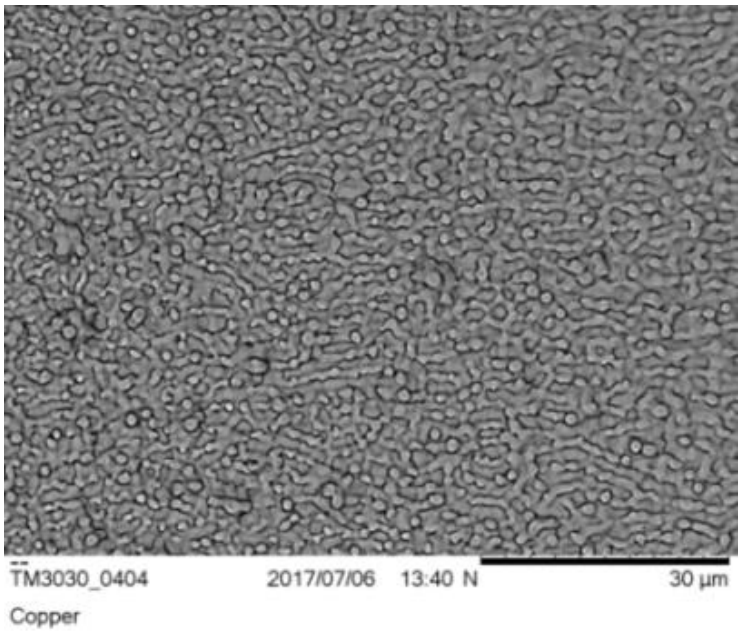

Fig. 11. Nanostructured copper surface (twofold processing) with an average contact angle of 115° (hydrophobic property). Nd3+:YAG crystal-laser's features: LW=532 nm; PE=0.14 J; PRR=10 Hz; PD=130 µs.

Experiment II-3.In this experiment titanium foil was taken as a sample, and for its laser processing the following characteristics of microsecond laser facility Nd^{3+}:YAG crystal were chosen:

- laser wavelength (LW): 532 nm;
- pulse energy (PE): 0.15 J;
- pulse repetition rate (PRR): 10 Hz;

– pulse duration (PD): 100 μs.

Results of a single pulse action on this sample are shown on the Fig. 12. The obtained nanostructured surface has a very good hydrophilic property with an average interfacial contact angle $\theta_{average} \approx 28°$, where both water and physiological solution NaCl 0.9% were used as the liquid.

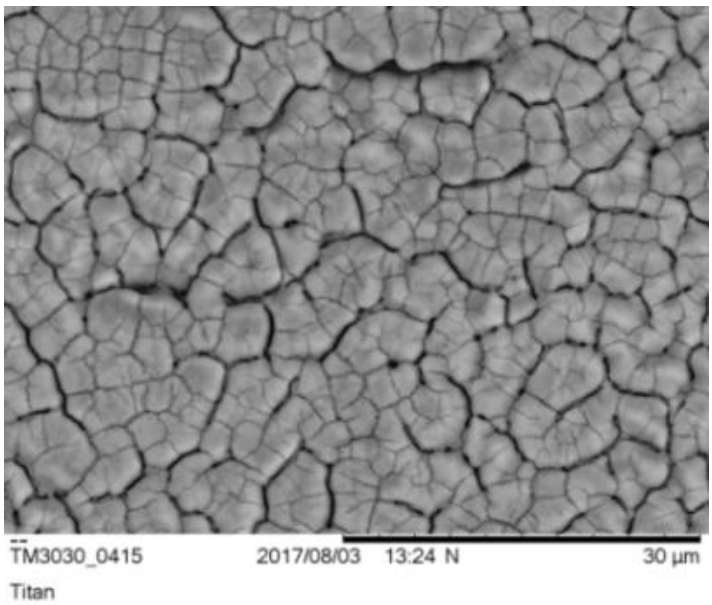

Fig. 12. Nanostructured titanium surface (one-time processing) with an average contact angle of 28° (very good hydrophilic property). Nd3+:YAG crystal-laser's features: LW=532 nm; PE=0.15 J; PRR=10 Hz; PD=100 μs.

Experiment II-4. In this experiment titanium foil was again taken as a sample, and for its laser processing the following characteristics of microsecond laser facility Nd^{3+}:YAG crystal were chosen:

– laser wavelength (LW): 532 nm;
– pulse energy (PE): 0.15 J;
– pulse repetition rate (PRR): 10 Hz;
– pulse duration (PD): 130 μs.

Results of a single pulse action on this sample are shown on the Fig. 13. The obtained nanostructured surface has a good hydrophilic property with an average interfacial contact angle $\theta_{average} \approx 42°$, however it is slightly worse, than in the results of the third experiment. In this experiment both water and physiological solution NaCl 0.9% was used as the liquid.

Experiment II-5.In this experiment titanium foil was again taken as a sample, and for its laser processing the following characteristics of microsecond laser facility Nd^{3+}:YAG crystal were chosen:

– laser wavelength (LW): 532 nm;
– pulse energy (PE): 0.15 J;
– pulse repetition rate (PRR): 10 Hz;
– pulse duration (PD): 85 μs.

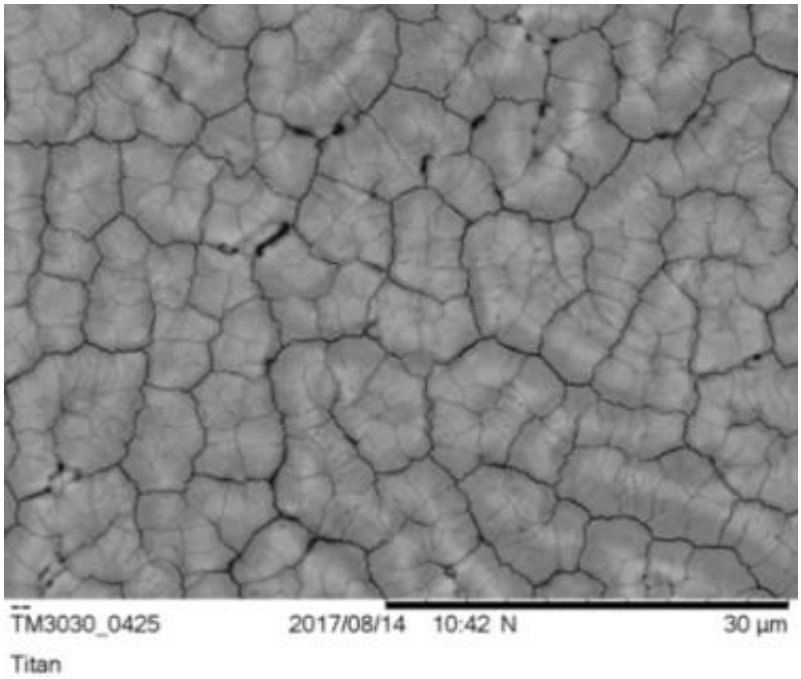

Fig. 13. Nanostructured titanium surface (one-time processing) with an average contact angle of 42° (good hydrophilic property). Nd3+:YAG crystal-laser's features: LW=532 nm; PE=0.15 J; PRR=10 Hz; PD=130 µs.

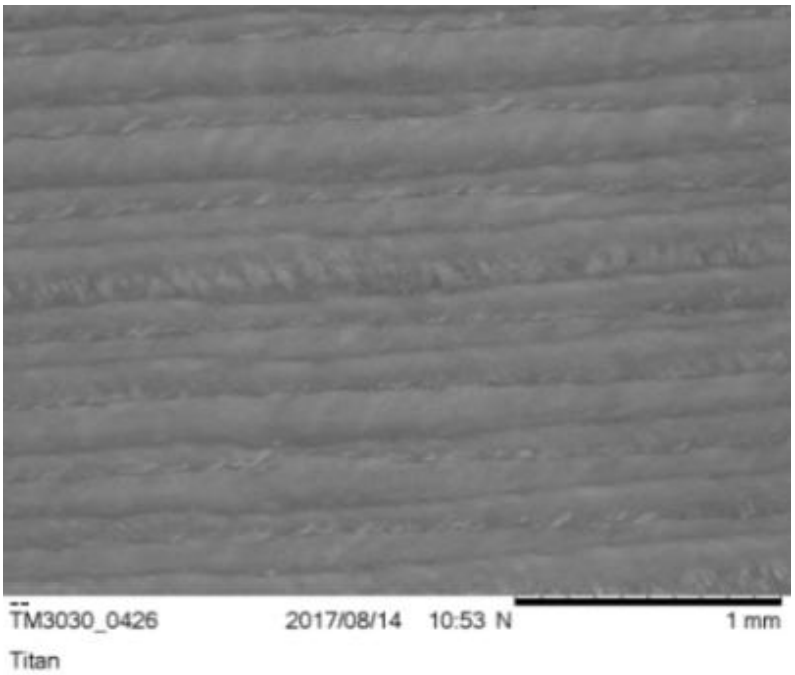

Fig. 14. Nanostructured titanium surface (one-time processing with a lens for focusing of a laser beam) with an average contact angle of 66° on processed strips: the liquid flows only in one direction. Nd3+:YAG crystal-laser's features: LW=532 nm; PE=0.15 J; PRR=10 Hz; PD=85 µs.

The processing was implemented by the stripes with use of a lens for focusing of laser beam. Results of a single pulse action on this sample are shown on the Fig. 14. The obtained nanostructured surface has the following hydrophilic property: the liquid

(both water and physiological solution NaCl 0.9%) flows only in one direction, and $\theta_{average} \approx \begin{cases} 66° & \text{on processed strips,} \\ 134° & \text{between processed strips.} \end{cases}$

Experiment II-6.In this experiment titanium foil was again taken as a sample, and for its laser processing the following characteristics of microsecond laser facility Nd^{3+}:YAG crystal were chosen:

- laser wavelength (LW): 532 nm;
- pulse energy (PE): 0.15 J;
- pulse repetition rate (PRR): 10 Hz;
- pulse duration (PD): 300 μs.

Results of a single pulse action on this sample are shown on the Fig. 15. The obtained nanostructured surface has a very good hydrophilic property with an average interfacial contact angle $\theta_{average} \approx 34°$, where both water and physiological solution NaCl 0.9% were used as the liquid.

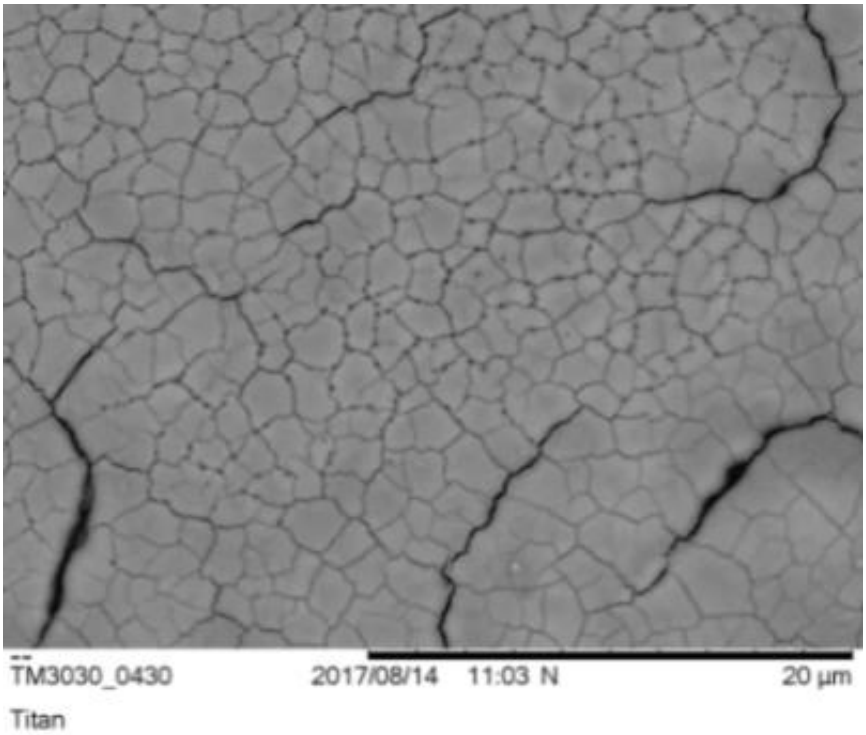

Fig. 15. Nanostructured titanium surface (one-time processing) with an average contact angle of 34° (very good hydrophilic property).Nd3+:YAG crystal-laser's features: LW=532 nm; PE=0.15 J; PRR=10 Hz; PD=300 μs.

5. Conclusion

This paper contains discusses about a relatively new direction related to the use of laser technology for surface treatment of biocompatible titanium implants in order to optimize its topography and physico-chemical properties. The brief overview of some of the results given in this paper demonstrates that laser treatment seems promising both in terms of providing a higher quality of the micromorphology of the surface of the material and in terms of increasing their corrosion resistance. It should be noted that the work aimed at improving the physical and chemical properties of the surface of titanium

implants by laser treatment is still at the initial stage of its development within the framework of application in orthopedics. For a deeper understanding of the nature of the change in surface properties under the influence of laser treatment, further investigations are needed with the use of modern surface-sensitive analytical methods that provide quantitative information at the atomic-molecular level.

In addition, in this paper it is proposed a mathematical model in terms of spherical trigonometry for describing the transfer of laser radiation in the surface treatment of the titanium head of the human hip joint endoprosthesis.

6. Acknowledgements

The authors express sincere gratitude to the colleague BS in Physics Uldis Zaimis from the Faculty of Science and Engineering, Liepaja University, Liepaja, Latvia, for the experiments carried out, as well as for providing us with the complete set of information about the obtained results.

For the first two co-authors the present article was executed within the framework of The State Research Programme "Next generation Information and Communication Technologies (NextIT)", Project No. 4.

References

1. Adamson, A.W., Gast, A.P. (1997). *Physical Chemistry of Surfaces*. New York, USA: John Wiley & Sons Publishing, 784 p.
2. Adell, R., Lekholm, U., Rockler, B., Branemark, P.-I. (1981). A 15-year study of osseointegrated implants in the treatment of the edentulous jaw. *International Journal of Oral Surgey*, 10(6), 387-416.
3. Ajdari, A. (1995). Electro-osmosis on inhomogeneously charged surfaces. *Physical Review Letters*, 75(4), 755-758.
4. Bakker, G. (1928). *Handbook on Experimental Physics. Volume 6: Capillarity and Surface Tension*. Leipzig, Germany: Akademische Verlagsgesellschaft, 458 p.
5. Barrat, J.L., Bocquet, L. (1999). Large slip effect at a nonwetting fluid-solid interface. *Physics Review Letters*, 82(23), 4671-4674.
6. Barret, P. (1973). *Kinetics of Heterogeneous Processes*. Paris, France: Gauthier-VillarsPublishing, 574 p.
7. Baxter, S., Cassie, A.B.D. (1945). The water repellency of fabrics and a new water repellency test. *Journal of the Textile Institute Transactions*, 36(4), 67-90.
8. Belyaev, A.V., Vinogradova, O.I. (2010). Effective slip in pressure-driven flow past superhydrophobic stripes. *Journal of Fluid Mechanics*, 652, 489-499.
9. Bhushan, B., Israelachvili, J.N., Landman, U. (1994). Nanotribology: friction, wear and lubrication at the atomic scale. *Nature: International Weekly Journal of Science*, 374(6523), 607-616.
10. Blkerman, J.J. (1978). Capillarity before Laplace: Clairaut, Segner, Monge, Young. *Archive for History of Exact Sciences*, 18(2), 103-122.
11. Branemark, P.-I., Hansson, B.O., Adell, R., Breine, U., Lindstrom, J., Hallen, O., Ohman, A. (1977). Osseointegrated implants in the treatment of the edentulous jaw. Experience from a 10-year period. *Scandinavian Journal of Plastic and Reconstructive Surgery and Hand Surgery*, 16, 1-132.
12. Cao, G. (2004). *Nanostructures and Nanomaterials: Synthesis, Properties, and Applications*. London, UK: Imperial College Press, 433 p.
13. Cardaioli, P., Giordan, M.,Rigatelli, G. (2007). Nickel allergy in interatrial shunt device-based closure patients, *Journal of Congenital Heart Disease*, 2(6), 416-420.

14. Cassie, A.B.D., Baxter, S. (1945). Large contact angles of plant and animal surfaces. *Nature*, 155, 21-22.
15. Choi, C.-H., Johan, K., Westin, A., Breuer, K.S. (2003). Apparent slip flows in hydrophilic and hydrophobic microchannels. *Physics of Fluids*, 15(10), 2897-2902.
16. Churaev, N.V., Derjaguin, B.V.,Muller, V.M. (1987). *Surface Forces*. Berlin, Germany: Springer-Verlag, 440 p.
17. Cottin-Bizonne, C., Barentin, C., Charlaix, E., Bocquet, L., Barrat, J. (2004). Dynamics of simple liquids at heterogeneous surfaces: Molecular-dynamic simulations and hydrodynamic description. *The European Physical Journal E*, 15(4), 427-438.
18. Deb, P. (2014). *Kinetics of Heterogeneous Solid State Processes*. New York, USA: SpringerPublishing, 49 p.
19. Delgado, M. (1997). The Lagrange-Charpit Method. *SIAM Review*, 39(2), 298-304.
20. Eletskii, A.V., Erkimbaev, A.O., Zitserman, V.Yu., Kobzev, G.A., Trakhtengerts, M.S. (2012). Thermophysical properties of nanoobjects: data classification and validity evaluation. *Journal of High Temperature*, *50*(4), 488-495.
21. Ferrara, M.C., Pilloni, L., Mazzarelli, S., Tapfer, L. (2010). Hydrophilic and optical properties of nanostructured titania Prepared by solgel-dip coating. *Journal of Physics D: Applied Physics*, *43*(9), 95301, 1-37.
22. Gelfand, I.M. (1959). Some problems of theory of quasi-linear equations. *Advances of Mathematical Sciences, Russian Mathematical Surveys*, *14*(2), 97-158.
23. General statistics about papers of P.-I. Branemark. [Online]. Available: http://scicurve.com/author/Br%C3%A5nemark%20P%20I [Accessed: November 13, 2017].
24. Gintsburg, A.L., Karyagina, A.S., Semikhin, A.S. (2011). Develepment of new generation of specimens for efficient repair of bone tissue. *Journal of Therapy and Prophylaxis*, 1, 80-84.
25. Gokhshtain, A.Ya. (1976). *Surface Tension of Solids and Adsorption*. Moscow, USSR: Science Publishing, 400 p.
26. Gong, Z., Wang, J., Wu, L., Wang, X., Lu, G., Liao, L. (2013). Fabrication of super hydrophobic surfaces on copper by solution-immersion. *Chinese Journal of Chemical Engineering*, *21*(8), 920-926.
27. Gurtin, M.E. (1996). Generalized Ginzburg-Landau and Cahn-Hilliard equations based on a microforce balance. *Journal of Physics D: Nonlinear Phenomena*, *92*(3-4), 178-192.
28. Hao, L., Lawrence, J. (2005). *Laser Surface Treatment of Bio-Implant Materials*. Chichester, UK: John Wiley & Sons Publishing, 211 p.
29. Hench, L.L. (1998). Bioceramics. *Journal of the American Ceramic Society*, 81, 1705-1728.
30. Hohenberg, P.C., Krekhov, A.P. (2015). An introduction to the Ginzburg-Landau theory of phase transitions and nonequilibrium patterns. *Journal of Physics Reports*, 572, 1-42.
31. Israelachvili, J.N. (1992). *Intermolecular and Surface Forces: With Applications to Colloidal and Biological Systems*. New York, USA: Academic Press, 450 p.
32. Kendall, K. (1994). Adhesion: molecules and mechanics. *Journal of Science*, 263(5154), 1720-1725.
33. Khasaya, R.R., Khomich, Y.V., Malinskiy, T.V., Mikolutskiy, S.I., Yamshchikov, V.A., Zheleznov, Y.A. (2014). Titanium surface processing by nanosecond laser radiation. *Letters on Materials*, *4*(1), 45-48.
34. Khomich, V.Yu.,Mikolutskiy, S.I., Shmakov, V.A., Yamschikov, V.A. (2012). Model of nanostructure formation on solid surface melted by laser pulse. In: *Proceedings of the International Conference on Nanomaterials: Application & Properties*, *1*(4), 04RES01, 1-4.
35. Khomich, V.Yu., Urlichich, Yu.M., Shmakov, V.A., Tokarev, V.N., Galstyan, A.M., Mikolutskiy, S.I., Malinskiy, T.V., Ganin, D.V. (2013). Formation of submicron structures

on the surface of Zirconium Dioxide under illumination of nanosecond laser. *Journal of Inorganic Materials: Applied Research*, *4*(3), 201-204.

36. Khomich, V.Yu., Shmakov, V.A. (2012). Formation of periodic nanodimensional structures on the surface of solids during phase and structural transformations. *Doklady Physics*, *57*(9), 349-351.
37. Kikoin, A.K., Kikoin, I.K. (1976). *Molecular Physics*. Moscow, USSR: Science Publishing, 478 p.
38. Labuntsov, D.A., Yagov, V.V. (1977). *Hydrodynamic Equilibrium and Wave Motions of Gas-liquid Systems*. Moscow, USSR: Moscow Power Engineering Institute Press, 72 p.
39. Landau, L.D., Lifshitz, E.M. (1987). *Course of Theoretical Physics. Volume 6: Fluid Mechanics*. Oxford, UK: Pergamon Press, 539 p.
40. Lauga, E., Stone, H.A. (2003). Effective slip in pressure-driven Stokes flow. *Journal of Fluid Mechanics*, 489, 55-77.
41. Majumder, A., Ghatak, A., Sharma, A. (2007). Microfluidic adhesion induced by subsurface microstructures. *Journal of Science*, *318*(5848), 258-261.
42. Mikolutskiy, S.I., Tokarev, V.N., Khomich, V.Yu., Shmakov, V.A., Yamshchikov,V.A. (2013). Investigation of Nanostructure formation on the surface of materials under the action of ArF-laser. *Journal of Advances of Applied Physics*, *1*(4), 548-553.
43. Nischenko, M.M., Shevchenko, N.A., Schur, D.V., Bogolepov, V.A., Dubovoi, A.G., Sidorchenko, I.M. (2010). Laser-stimulated emission of electrons from carbon nanostructures formed at laser evaporation of oriented carbon nanotubes.*Journal of Inorganic Materials: Applied Research*, *1*(4), 276-278.
44. Novikov, N.V., Rozenberg, O.A., Gavlik, J., Sohan, S.V., Vozniy, V.V., Turmanidze, R.S., Buchrikidze, D.S., Beridze, M.D. (2011). *Implants of Human Joints: Materials and Technologies*. Kiev, Ukraine: Bakul Institute for Superhard Materials Press, 528 p.
45. Oner, D. (2001). Ultrahydrophobic surfaces: effects of topography length scales on wettability. *Dissertation to obtaining the scientific degree PhD*, Graduate School of the University of Massachusetts Amherst, Amherst, MA, USA, 135 p.
46. Oner, D., McCarthy, T.J. (2000). Ultrahydrophobic surfaces. Effects of topography length scales on wettability. *Langmuir*, *16*(20), 7777-7782.
47. Ono, S., Kondo, S. (1960). Molecular Theory of Surface Tension in Liquids. In: *Structure of Liquids. Encyclopaedia of Physics*. Berlin-Heidelberg: Springer-Verlag, *3*(3), 134-280.
48. Oshida, Y. (2013). *Bioscience and Bioengineering of Titanium Materials*. Waltham, USA: Elsevier Publishing, 500 p.
49. Ou, J., Rothstein, J.P. (2005). Direct velocity measurements of the flow past drag-reducing ultrahydrophobic surfaces. *Physics of Fluids*, 17, 103606, 1-10.
50. Palmer, C.I., Leigh, C.W. (1934). *Plane and Spherical Trigonometry*. New York & London: McGraw-Hill Book Company, 229 p.
51. Pomogailo, A.D., Kestelman, V.N. (2005). *Metallopolymer Nanocomposites*. Berlin-Heidelberg, Germany: Springer-Verlag Publishing, 564 p.
52. Puz, A.V. (2014). Multifunctional Coatings for alloys of medical purpose. *Doctoral Thesis*, Institute of Chemistry, Far Eastern Department of the Russian Academy of Sciences, 164 p.
53. Remeeva, E.A., Rozanova, I.B., Elinson, V.M., Sevastianov, V.I. (2003). Influence of biomaterials surface on platelets release ATP in vitro. *International Journal of Artificial Organs*, *26*(7), 634-639.
54. Rios, P.F., Dodiuk, H., Kenig, S., McCarthy, S., Dotan, A. (2006). The effects of nanostructure and composition on the hydrophobic properties of solid surfaces. *Journal of Adhesion Science and Technology*, *20*(6), 563-587.
55. Rozenberg, O.A., Sokhan, S.V., Vozny, V.V., Mamalis, A.G., Gavlik, J., Kim, D.-J. (2006). Trends and development in the manufacturing of hip joints: an overview. *International Journal of Advanced Manufacturing Technology*, 27, 537-542.
56. Rusanov, A.I., Goodrich,F.C. (1980). *The Modern Theory of Capillarity: The Centennial Gibbs' Theory of Capillarity*. Leningrad, USSR: Chemistry Publishing, 344 p.

57. Sarra, S.A. (2003). The method of characteristics with applications to conservation laws. *Journal of Online Mathematics and its Applications*, 3, 1-16.
58. Steinberger, A., Cottin-Bizonne, C., Kleimann, P., Charlaix, E. (2007). High friction on a bubble mattress. *Nature Materials*, 6, 665-668.
59. Takemoto, S., Kusudo, Y., Tsuru, K., Hayakawa, S. (2004). Selective protein adsorption and blood compatibility of hydroxy-carbonate apatites. *Journal of Biomedical Materials Research*, *69A*(3), 544-551.
60. Tikhonov, A.N., Arsenin, V.Ya. (1977). *Solution of Ill-posed Problems*. Washington, USA: Winston & Sons Publishing, 258 p.
61. Titanium alloy. [Online]. Available: https://en.wikipedia.org/wiki/Titanium_alloy [Accessed: November 13, 2017].
62. Tokarev, V.N., Shmakov, V.A., Khomich, V.Yu., Khasaya, R.R., Mikolutsky, S.I., Nebogatkin, S.V., Yamschikov,V.A. (2010). Review of Methods of Direct Laser Nanostructuring Technological Materials. In: *Proceedings of the 29th International Congress on Applications of Lasers and Electrooptics*, 1257-1265.
63. Traini, T., Berardini, M., Congedi, F., Sinjari, B., Trisi, P., Caputi, S. (2017). Impact of second stage surgery on bone remodeling around new hybrid titanium implants: A Prospective Clinical Study in Humans. *Journal of Implant Dentistry*, *26*(1), 121-128.
64. Trisi, P., Berardini, M., Colagiovanni, M., Berardi, D., Perfetti, G.L. (2016). Laser-treated titanium implants: an in vivo histomorphometric and biomechanical analysis. *Journal of Implant Dentistry*, *25*(5), 575-580.
65. Turmanidze, R.S., Aptsiauri, T.S., Popkhadze, G.Z. (2015). New materials for implants of the human hip joint and technology of their machining with the achievement of high precision and quality of spherical surfaces. *Journal of Mechanical Engineering*, *75*(3), 64-71.
66. Vasilev, M.A., Chenakin, S.P., Nishchenko, M.M., Yatsenko, L.F. (2015). Effect of pulsed laser radiation to the composition of the surface layers of the titanium alloy VT6. *Journal of Metal Physics and Advanced Technologies*, *37*(7), 861-870.
67. Vasilev, M.A., Nischenko, M.M., Gurin, P.A. (2010). Laser modification of surface of titanium implants. *Progresses of Physical Metallurgy*, 11, 209-247.
68. Ventsel, M.K. (1934). *Spherical Trigonometry*. Moscow, USSR: GeodezIzdat, 154 p.
69. Vinogradova, O.I., Yakubov, G.E. (2006). Surface roughness and hydrodynamic boundary conditions. *Physical Review E*, *73*(4), 045302(R), 1-4.
70. Wang, G., Zraigat, H. (2010). Functional coatings or films for hard-tissue applications. *Journal of Materials*, *3*(7), 3994-4050.
71. Wenzel, R.N. (1936). Resistance of solid surfaces to wetting by water. *Industrial and Engineering Chemistry Research*, *28*(8), 988-994.
72. Ybert, C., Barentin, C., Cottin-Bizonne, C., Joseph, P., Bocquet, L. (2007). Achieving large slip with superhydrophobic surfaces: Scaling laws for generic geometries. *Physics of Fluids*, 19, 123601, 1-10.
73. Zaimis, U., Guseynov, Sh.E. (2017). Scientifically substantiated guidelines for physico-mathematical modelling of Laser Surface-treatment of Wear-resistant Implants for Human Joint Replacements. In: *Proceedings of the 11th International Scientific and Practical Conference "Environment. Technology. Resources"*, 3, 350-356.
74. Zimon, A.D. (1974). *Fluid Adhesion and Wetting*. Moscow, USSR: Chemistry Publishing, 416 p.